

Model absorption potential for electron-molecule scattering in the intermediate-energy range

M.-T. Lee,¹ I. Iga,¹ L. E. Machado,² and L. M. Brescansin³

¹*Departamento de Química, UFSCar, 13565-905 São Carlos, São Paulo, Brazil*

²*Departamento de Física, UFSCar, 13565-905, São Carlos, São Paulo, Brazil*

³*Instituto de Física “Gleb Wataghin,” UNICAMP, 13083-970 Campinas, São Paulo, Brazil*

(Received 27 April 2000; published 9 November 2000)

Calculated elastic differential, integral, and momentum transfer cross sections as well as total (elastic + inelastic) cross sections for electron-CH₄ collisions are reported in the (20–500)-eV energy range. Four model potentials of both a nonempirical and semiempirical nature are used to represent absorption effects. The Schwinger variational iterative method combined with the distorted-wave approximation is used to solve the scattering equations. Through the comparison of our calculated results with available experimental data, two of these model absorption potentials are recommended as more convenient for treating electron-molecule collision problems.

PACS number(s): 34.80.Bm

I. INTRODUCTION

Recently, there has been significant progress in the development of both theoretical and computational methods for studies on the dynamics of electron-molecule collision processes. In the present, elastic cross sections, shape-resonance positions, as well as Ramsauer-Townsend minima for collisions of low-energy electrons with small polyatomic molecules can be accurately predicted using an interaction potential consisting of an exact static-exchange part plus polarization contributions, which can be obtained either via *ab initio* methods [1,2] or via parameter-free local electronic density distribution models [3–5]. Nevertheless, when such approximations are used to study elastic electron-molecule scattering in the intermediate energy range (from ionization threshold to a few hundreds eV), the calculated differential cross sections (DCS's) usually lie significantly above the measured data, particularly at intermediate and large scattering angles. The reason for this discrepancy is the well-known existence of absorption effects [6]: at impact energies above excitation and ionization thresholds, the flux of the scattered electrons is distributed over all the open channels, consequently resulting in a reduction of the flux corresponding to the elastic scattering.

Although the main features of the absorption effects are known, taking these effects into account in an *ab initio* treatment of electron-molecule scattering is a very difficult task. For instance, close-coupling calculations would have all discrete and continuum open channels included in the open-channel P space, which would make the calculations computationally unfeasible. Therefore, the use of model absorption potentials seems to be presently the only practical manner for treating electron-atom and electron-molecule collisions in the intermediate energy range. Indeed, several model absorption potentials of both empirical [7–9] and nonempirical [10,11] natures for electron-atom scattering have been proposed for more than 20 years. Among these model potentials, the quasifree scattering model (QFSM) proposed by Staszewska *et al.* [11] is particularly interesting. The QFSM was derived nonempirically to reproduce the absorption probability per unit time for an electron passing through a free-

electron gas, where the electron-electron absorption cross sections are calculated using the Pauli-allowed binary-encounter approximation. The target is modeled locally as a free-electron gas (FEG) with Fermi momentum k_F depending on the density. Lately, the QFSM was modified empirically by Staszewska *et al.* [12] in order to introduce some target properties, such as ionization potentials and threshold excitation energies, into the collisional dynamics. Although some modified versions of that method have been presented, two of them, namely the versions 2 (STV2) and 3 (STV3) of QFSM, are the most successful. With those modifications, the agreement between theory and experiment is improved, but the method loses its *ab initio* nature. On the other hand, the use of semiempirical QFSM versions does not require any parameters to be adjusted for a given target and for a given incident energy. Therefore, it is easy to use and can provide cross sections for predictive purposes, rather than just for correlation and interpolation of a preexisting data basis. In fact, a modified version of the STV3 (to be referred to as JB3 below) has been successfully applied by our group to study the electron scattering by N₂ [13], CO₂ [14], and CH₄ [15] in the intermediate energy range. Very recently, however, Blanco and García [16] have identified and corrected an error in the derivation of the original version of QFSM of Staszewska *et al.* [11]. Furthermore, some improvements on the QFSM were also suggested by Blanco and García. Nevertheless, their model absorption potential has not yet been sufficiently tested.

In view of the presence of various nonempirical and semiempirical versions of QFSM in the literature, it is interesting to verify how each of these versions works in an actual cross-section calculation for electron-molecule collisions. In this work, we report a systematic study on the electron-CH₄ scattering in the (20–500)-eV energy range. As an extension of our previous work [15], various versions of QFSM are used here to represent the absorption effects. Through the comparison of calculated results with experimental data, we expect to find a more effective version for the study of electron-molecule scattering in the intermediate energy range. Because of the existence of a large amount of experimental data in the literature [17–24], electron scattering by

methane is chosen for this purpose.

The organization of this paper is as follows. In Sec. II, we briefly describe various QFSM versions and some details of the calculation. In Sec. III, we compare our calculated results with the existing experimental data.

II. THEORY AND CALCULATION

A. The QFSM of Staszewska *et al.*

The absorption potential in the QFSM versions is given by

$$V_{ab}(\vec{r}) = -\frac{1}{2}\rho(\vec{r})v_{\text{loc}}\bar{\sigma}_b, \quad (1)$$

where $v_{\text{loc}}(\vec{r}, E)$ is the local speed of an incident electron, given by

$$v_{\text{loc}}(\vec{r}, E) = [2(E - V^{\text{SE}})]^{1/2}. \quad (2)$$

In Eqs. (1) and (2), V^{SE} is the static-exchange potential, $\rho(\vec{r})$ is the target electronic density, and $\bar{\sigma}_b$ is the average binary-encounter cross section for electron-electron collisions. This quantity is obtained by averaging the Rutherford cross sections over a free-electron gas of density $\rho(\vec{r})$ subjected to the constraints

$$k^2 \geq \alpha, \quad (3)$$

$$p^2 \geq \beta, \quad (4)$$

where k and p are the final momenta of the bound and scattering electrons, respectively, and α and β are model-dependent parameters defined below. A semiclassical correction factor of $\frac{1}{2}$ is introduced to approximately account for the effects of exchange. The resulting cross section is given by

$$\bar{\sigma}_b(\vec{r}, E) = \frac{32\pi^2 N_k}{15p^2} (f_1 + f_2) H(p^2 - \alpha - \beta + k_F^2), \quad (5)$$

where

$$N_k(\vec{r}) = \frac{3}{4\pi k_F^3}, \quad (6)$$

$$p(E) = (2E)^{1/2}, \quad (7)$$

$$f_1(\vec{r}, E) = \frac{5k_F^3}{(\alpha - k_F^2)} - \frac{k_F^3[5(p^2 - \beta) + 2k_F^2]}{(p^2 - \beta)^2}, \quad (8)$$

$$f_2(\vec{r}, E) = 2H(\alpha + \beta - p^2) \frac{(\alpha + \beta - p^2)^{5/2}}{(p^2 - \beta)^2}, \quad (9)$$

$$k_F = [3\pi^2 \rho(\vec{r})]^{1/3}. \quad (10)$$

In Eqs. (5)–(10), $p(E)$ is the incident momentum of the scattering electron, k_F is the target Fermi momentum, and $H(x)$ is a Heaviside function defined by $H(x) = 1$ for $x \geq 0$ and $H(x) = 0$ for $x < 0$.

In the original QFSM version (STV1), α and β are given by

$$\alpha(\vec{r}, E) = k_F^2 - \Delta, \quad (11)$$

$$\beta(\vec{r}, E) = k_F^2, \quad (12)$$

where Δ is the threshold excitation energy.

On the other hand, in STV2,

$$\alpha(\vec{r}, E) = k_F^2 + \Delta - V^{\text{SE}}, \quad (13)$$

$$\beta(\vec{r}, E) = \alpha; \quad (14)$$

and in STV3,

$$\alpha(\vec{r}, E) = k_F^2 + 2[\Delta - (I - \Delta)] - V^{\text{SE}}, \quad (15)$$

$$\beta(\vec{r}, E) = k_F^2 + 2(I - \Delta) - V^{\text{SE}}, \quad (16)$$

where I is the ionization potential.

B. The modified version of Jain and Baluja

In 1992, Jain and Baluja [25] reported a total (elastic plus inelastic) cross section (TCS) calculation for a large number of molecules. In their study, they employed a model absorption potential (JB2) which is a modified version of STV2 given as

$$V_{ab}(\vec{r}) = -\frac{1}{2}\rho(\vec{r})[T_{\text{loc}}/2]^{1/2}\bar{\sigma}_b, \quad (17)$$

where $\rho(\vec{r})$ and $\bar{\sigma}_b$ have the same meaning as in STV2, while

$$T_{\text{loc}} = p^2 - 2V^{\text{SEP}}, \quad (18)$$

V^{SEP} being the static-exchange-polarization potential. Also, Δ in JB2 is the mean excitation energy of the target instead of the threshold excitation energy. More recently, the JB2 and STV3 models have been combined [13], resulting in a new version of the semiempirical absorption potential that will be referred to as JB3. JB3 has the same form as JB2, except that the definition of α and β follows STV3.

C. The modified versions of Blanco and García

Very recently, Blanco and García [16] have reviewed the derivation of the original QFSM and found an error in it. The corrected absorption potential in the version that we will refer to as BG1 is exactly that of the original STV1, divided by 2. Furthermore, an additional term based on the Mott scattering formula has been introduced by Blanco and García, which has the form

$$V_C = \frac{2u}{\pi p} H(p^2 - k_F^2 - 2\Delta) [f_\delta(k_F/p) - f_\delta(H(\delta)\delta^{1/2})], \quad (19)$$

where u is the local speed of the scattering electron, given by

$$u = [2(E - V^{\text{SEP}})]^{1/2}, \quad (20)$$

$$\delta(\vec{r}, E) = \frac{2(k_F^2 + \Delta)}{p^2} - 1, \quad (21)$$

and

$$f_\delta(x) \cong \frac{x(1-\delta)}{4(1-x)} + \frac{1}{16} [11-x+(x-3)\delta] \log_{10}(1-x) + (a_1 - \delta b_1)x + (a_2 - \delta b_2)x^2, \quad (22)$$

with $a_1 = 0.4353$, $a_2 = 0.01233$, $b_1 = -0.1084$, and $b_2 = 0.05691$. We will refer to the potential model with Mott scattering correction as BG2.

In addition, Blanco and García [16] have also attempted to account for the screening of the inner electrons by the outmost ones. They have suggested the replacement of the local speed (u) by the incident speed (p) in all the final potential expressions. Nevertheless, we have verified that this change affects only slightly the calculated cross sections and thus will not be considered in the present study.

D. Some details of the calculation

The details of the calculation have been published elsewhere [15], so only a brief discussion of the calculations will be presented here. Within the fixed-nuclei framework, the electron-molecule scattering dynamics is represented by a complex optical potential, given by

$$V_{\text{opt}}(\vec{r}) = V^{\text{SEP}}(\vec{r}) + iV_{ab}(\vec{r}), \quad (23)$$

where V^{SEP} is the real part of the interaction potential formed by the static (V_{st}), the exchange (V_{ex}), and the correlation-polarization (V_{cp}) contributions. In our calculation, V_{st} and V_{ex} are derived exactly from a self-consistent-field (SCF) target wave function, while V_{cp} is derived, in the framework of FEG, from a parameter-free local density as prescribed by Padiál and Norcross [26]. Four versions of model potentials, namely STV3, JB3, BG1, and BG2, were used to represent the absorption effects.

In the two-potential formalism, the interaction potential is split as

$$V_{\text{opt}} = U_1 + U_2, \quad (24)$$

where U_1 is taken as the real part of the complex optical potential, whereas U_2 is the imaginary absorption potential. The corresponding distorted wave functions satisfy the following scattering equation:

$$(H_0 + U_1 - E)\chi = 0, \quad (25)$$

which is solved using the Schwinger variational iterative method (SVIM) [27]. Furthermore, the absorption part of the T matrix is calculated via the distorted-wave approximation (DWA) [28,29] as

$$T_{ab} = i \langle \chi_f^- | V_{ab} | \chi_i^+ \rangle, \quad (26)$$

where the superscripts (\pm) denote the incoming-wave and outgoing-wave boundary conditions.

In our study, U_1 is derived from the ground-state wave function of methane. This one-determinant near-Hartree-Fock wave function is composed of linear combination of atomic orbitals molecular spin orbitals that are calculated using the same contracted Cartesian Gaussian basis set as in Ref. [15]. At the equilibrium C-H bond distance ($R_{\text{C-H}} = 2.0503a_0$) this basis set gives a SCF energy of -40.1987 a.u. which can be compared with the -40.2155 a.u., value of Nishimura and Itikawa [30]. V_{cp} is constructed using the electronic density given by the SCF wave function. The asymptotic form of this potential is given (for T_d molecules) by

$$V_{\text{cp}}(\vec{r}) = -\frac{1}{2} \frac{\alpha_0}{r^4}, \quad (27)$$

where α_0 is the spherical part of the molecular dipole polarizability. In our calculations, the experimental value $\alpha_0 = 17.5$ a.u. was taken [31]. The parameters l and Δ used for generating the absorption potentials were taken from Jain and Baluja [25].

Furthermore, both the target bound orbitals and the static potential are partial-wave expanded in terms of symmetry-adapted basis functions. These expansions are truncated at some cutoff parameters $l_c = 16$ and $h \leq l$ for a given l . With this cutoff, the normalization of all bound orbitals is better than 0.999. In SVIM calculations, we have also limited the partial-wave expansions to $l_c = 16$. Additional terms which account for the contributions of angular momenta higher than l_c are included in the scattering amplitude calculation as follows:

$$f(\hat{k}', \hat{k}_0) = \sum_{l, h, l', h'}^{l_c, l'_c} f_{l, h, l', h'} + f^{(\text{higher})}, \quad (28)$$

where

$$f^{(\text{higher})} = \frac{1}{2ik} \sum_{l=l_c+1}^{l_{\text{max}}} (2l+1)(e^{2i\delta_l} - 1) P_l(\cos \theta) \quad (29)$$

and δ_l is the partial-wave phase shift, given by a closed formula:

$$\tan \delta_l = -\frac{\pi k^2 \alpha_0}{(2l-1)(2l+1)(2l+3)}. \quad (30)$$

In this work, terms with angular momentum phase shifts up to $l_{\text{max}} = 200$ were used in Eq. (29).

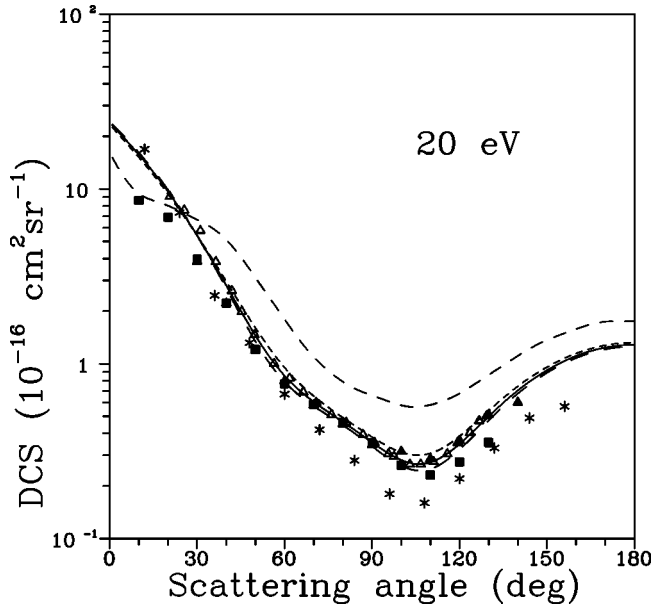


FIG. 1. DCS's for elastic e^- -CH₄ collision at 20 eV. Solid line, calculated results using JB3; short-dashed line, calculated results using BG1; dashed line, calculated results using BG2; long-dashed line, calculated results using STV3; full triangles, experimental data of Curry *et al.* [17]; open triangles, experimental data of Vuskovic and Trajmar [19]; full squares, experimental data of Boesten and Tanaka [22]; asterisks, experimental data of Shyn and Cravens [21].

The DCS's and ICS's for elastic electron-CH₄ scattering are calculated by the usual manner [32]. Moreover, the total cross sections (TCS's) are obtained via the optical theorem:

$$\sigma_{\text{tot}} = \frac{4\pi}{k} \text{Im} f(\hat{k}' = 0). \quad (31)$$

III. RESULTS AND DISCUSSION

In Figs. 1–6 we compare our calculated DCS's for elastic e^- -CH₄ scattering using STV3, JB3, BG1, and BG2 with some selected experimental data at incident energies of 20, 50, 100, 200, 300, and 500 eV, respectively. At 20 eV, the calculated results using STV3, JB3, and BG1 agree very well with each other. On the other hand, the DCS's obtained using BG2 are in general overestimated. With the increase of the incident energy, although the calculated DCS's using these model potentials still agree well with each other at small scattering angles, the discrepancy among them at large angles becomes more significant. At 50 eV, there is a good agreement between the results calculated with JB3 and BG1 and with the experimental data. The calculated DCS's using BG2 lie again systematically above the measured data, while the DCS's from STV3 lie below. At 100 eV, good agreement is seen between the DCS's of JB3 and BG2 and the experimental data while the results of STV3 and BG1 lie below. Above 100 eV, the discrepancies between the results calculated using JB3 and STV3 become smaller with increasing incident energies and both agree well with the experiments. On the other hand, the results obtained using BG1 and BG2 lie systematically below the experimental data. In addition,

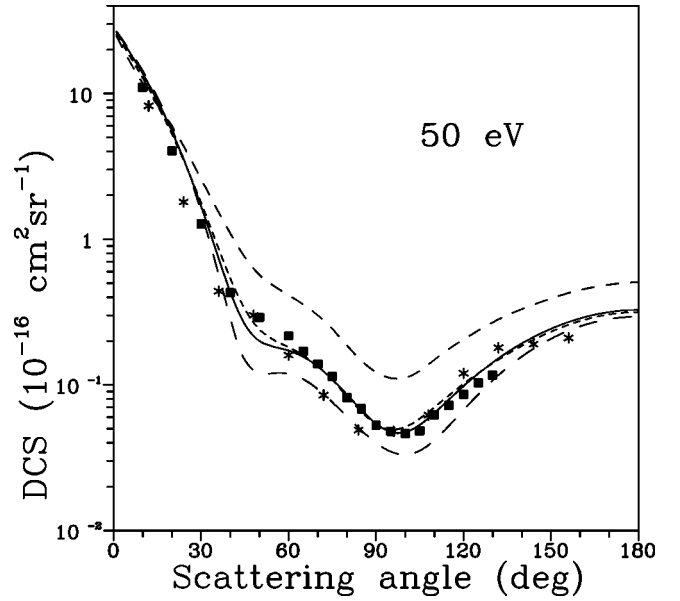


FIG. 2. Same as Fig. 1, but for 50 eV. The symbols are the same as in Fig. 1.

unphysical oscillations are seen in the DCS's calculated with BG2 for energies of 200 eV and above. Such oscillations are also present in the BG1 results at 500 eV.

Figures 7 and 8 compare the calculated ICS's and MTCS's, respectively, for elastic e^- -CH₄ scattering in the (20–500)-eV energy range using STV3, JB3, BG1, and BG2 with some selected experimental data [15,21,22,33]. The calculated ICS's using the four model potentials agree very well with each other for incident energies above 80 eV. This is somehow expected since the large-angle scattering contributions to ICS's are not important in the energy range of hundreds of eV. On the other hand, they contribute significantly

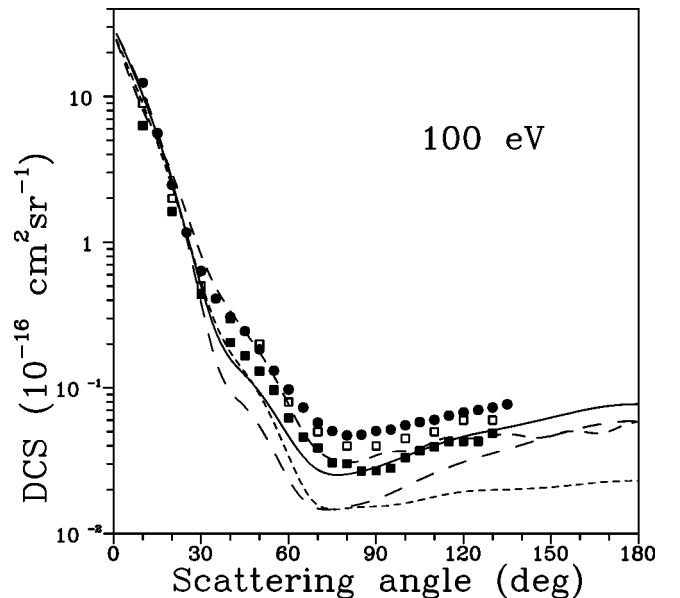


FIG. 3. Same as Fig. 1, but for 100 eV. The symbols are the same as in Fig. 1, except full circles, experimental results of Iga *et al.* [15]; open squares, experimental data of Sakae *et al.* [33].

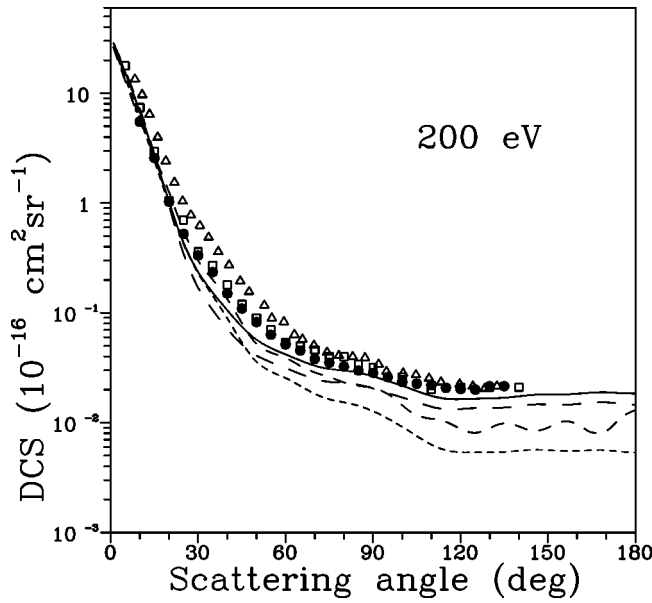


FIG. 4. Same as Fig. 3, but for 200 eV.

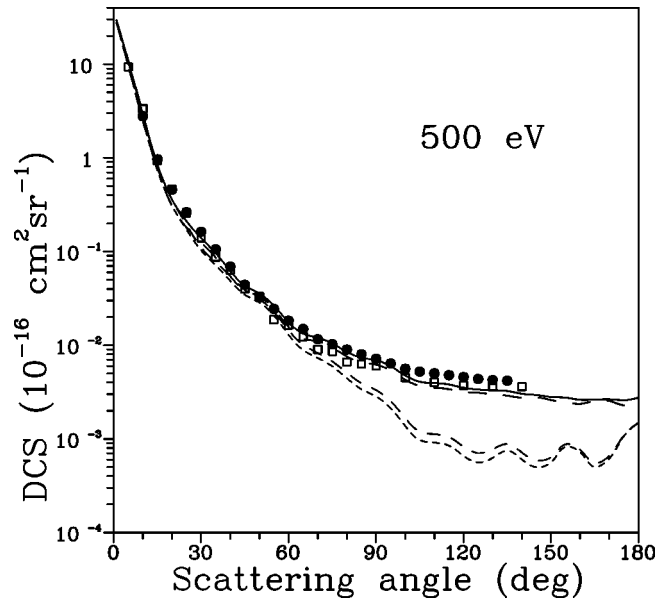


FIG. 6. Same as Fig. 3, but for 500 eV.

to MTCS's. It is shown in Fig. 8 that the calculated MTCS's of JB3 agree very well with the experimental data in the entire energy range covered herein, while the results of other model potentials underestimate the MTCS's at higher incident energies. Nevertheless, BG2 overestimates both the ICS's and MTCS's at lower incident energies.

In Fig. 9, we show our calculated TCS's using the above four model potentials in the (20–500)-eV energy range along with some selected experimental data [34–37]. All calculations underestimate the TCS's at higher incident energies. This is in accordance with early studies of Staszewska *et al.* [12] on electron scattering by rare gases and shows that this discrepancy is inherent to the proposed model potential. Despite that, the TCS's obtained by the STV3 are still in reasonable agreement with the experiments in the entire en-

ergy range, followed by those of JB3. On the other hand, the TCS's calculated using BG2 lie systematically below experimental and other calculated data. In particular, at incident energies below 100 eV, the BG2 TCS's are smaller than the corresponding ICS's reflecting the contribution of unphysical negative absorption cross sections.

In summary, we report calculated elastic DCS's, ICS's, and MTCS's as well as TCS's for e^- -CH₄ scattering in the (20–500)-eV incident energy range using four different formulations of absorption model potentials based on QFSM. Our study has revealed that, in general, the cross sections calculated using the semiempirical versions JB3 and STV3

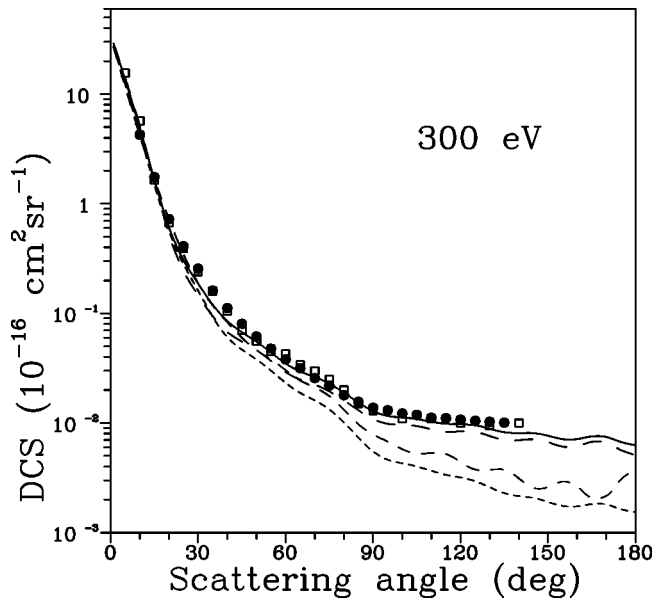


FIG. 5. Same as Fig. 3, but for 300 eV.

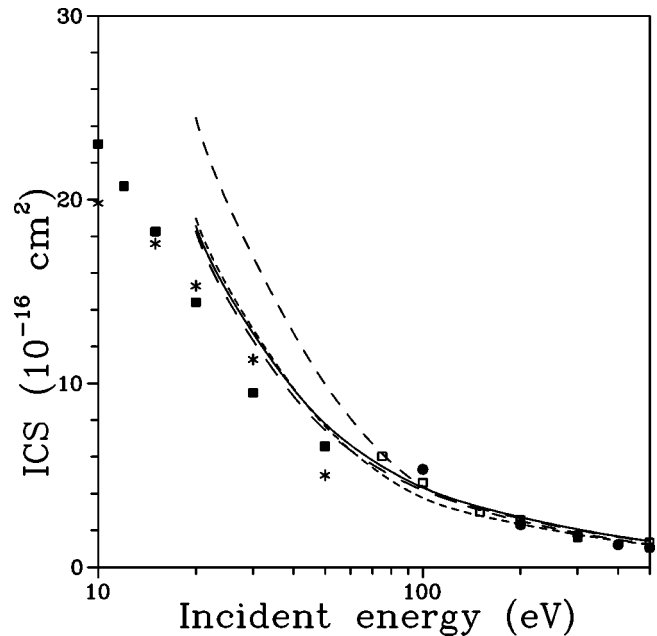


FIG. 7. ICS's for elastic e^- -CH₄ collision in the (10–500)-eV energy range. The symbols are the same as Fig. 3.

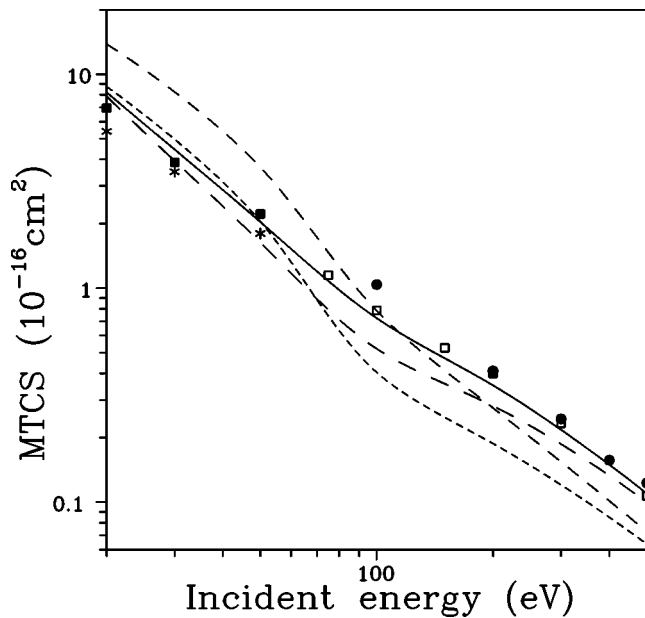


FIG. 8. MTCS's for elastic e^- -CH₄ collision in the (10–500)-eV energy range. The symbols are the same as in Fig. 3.

are in better agreement when compared with experiments. In particular, the use of JB3 leads to better results than STV3 in the calculation of elastic DCS's, ICS's, and MTCS's, whereas STV3 provides more reliable TCS's. On the other hand, the nonempirical version BG1 fails mainly at higher incident energies while BG2 can even yield unphysical negative absorption cross sections. Therefore, despite the loss of the *ab initio* nature, the application of JB3 and STV3 to electron-molecule scattering is still very convenient since it can provide reliable cross sections and does not require any parameter to be adjusted for a given target and for a given

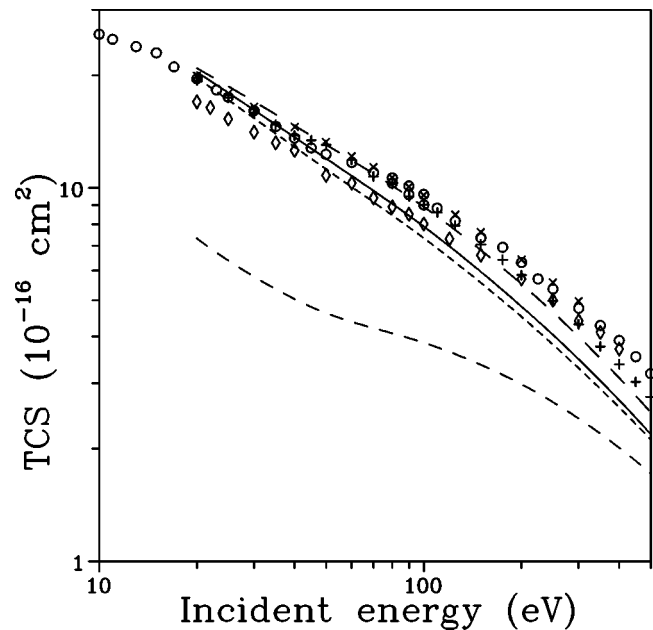


FIG. 9. TCS's for elastic e^- -CH₄ collision in the (10–500)-eV energy range. The symbols are the same as in Fig. 3 except open circles, experimental results of Zecca *et al.* [34]; pluses, experimental results of Nishimura and Sakae [35]; open diamonds, experimental results of Sueoka and Mori [36]; crosses, experimental results of Kanik *et al.* [37].

incident energy. Some preliminary results on electron-N₂O scattering [38] have also led to the same conclusions. Similar studies on other molecular systems are underway.

ACKNOWLEDGMENTS

The present work was partially supported by the Brazilian agencies FAPESP, CNPq, and FINEP-PADCT.

- [1] B.H. Lengsfeld III, T.N. Rescigno, and W.C. McCurdy, *Phys. Rev. A* **44**, 4296 (1991).
- [2] B.N. Nestmann, K. Pfingst, and S.D. Peyerimhoff, *J. Phys. B* **27**, 2297 (1994).
- [3] P. McNaughten, D.G. Thompson, and A. Jain, *J. Phys. B* **23**, 2405 (1990).
- [4] F.A. Gianturco, J.A. Rodrigues-Ruiz, and N. Sanna, *J. Phys. B* **28**, 1287 (1995).
- [5] L.E. Machado, M.-T. Lee, and L.M. Brescansin, *Braz. J. Phys.* **28**, 111 (1998).
- [6] C.J. Joachain, *Quantum Collision Theory* (North-Holland Publishing Co., Amsterdam, 1975).
- [7] I.E. McCarthy, C.J. Noble, B.A. Phillips, and A.D. Turnbull, *Phys. Rev. A* **15**, 2173 (1977).
- [8] A.E.S. Green, D.E. Rio, and T. Ueda, *Phys. Rev. A* **24**, 3010 (1981).
- [9] D. Thirumalai and D.G. Truhlar, *Phys. Rev. A* **26**, 793 (1982).
- [10] C.J. Joachain, K.H. Vanderpoorten, K.H. Winters, and F.W. Byron, Jr., *J. Phys. B* **10**, 227 (1977).
- [11] G. Staszewska, D.W. Schwenke, D. Thirumalai, and D.G. Truhlar, *Phys. Rev. A* **28**, 2740 (1983).
- [12] G. Staszewska, D.W. Schwenke, and D.G. Truhlar, *Phys. Rev. A* **29**, 3078 (1984).
- [13] M.-T. Lee and I. Iga, *J. Phys. B* **32**, 453 (1999).
- [14] I. Iga, M.G.P. Homem, K.T. Mazon, and M.-T. Lee, *J. Phys. B* **32**, 4373 (1999).
- [15] I. Iga, M.-T. Lee, M.G.P. Homem, L.E. Machado, and L.M. Brescansin, *Phys. Rev. A* **61**, 22708 (2000).
- [16] F. Blanco and A. García, *Phys. Lett. A* **255**, 147 (1999).
- [17] P.J. Curry, S. Newell, and A.C. Smith, *J. Phys. B* **18**, 2303 (1985).
- [18] H. Tanaka, T. Okada, L. Boesten, T. Suzuki, T. Yamamoto, and M. Kubo, *J. Phys. B* **15**, 3305 (1982).
- [19] L. Vuskovic and S. Trajmar, *J. Chem. Phys.* **78**, 4947 (1983).
- [20] W. Sohn, K.-H. Kochem, K.-M. Scheuerlein, K. Jung, and H. Ehrhardt, *J. Phys. B* **19**, 3625 (1986).
- [21] T.W. Shyn and T.E. Cravens, *J. Phys. B* **23**, 293 (1990).
- [22] L. Boesten and H. Tanaka, *J. Phys. B* **24**, 821 (1991).
- [23] I. Kanik, S. Trajmar, and J.C. Nickel, *J. Geophys. Res., [Planet.]* **98**, 7447 (1993).

- [24] B. Mapstone and W.R. Newell, *J. Phys. B* **25**, 491 (1992).
- [25] A. Jain and K.L. Baluja, *Phys. Rev. A* **45**, 202 (1992).
- [26] N.T. Padial and D.W. Norcross, *Phys. Rev. A* **29**, 1742 (1984).
- [27] R.R. Lucchese, G. Raseev, and V. McKoy, *Phys. Rev. A* **25**, 2572 (1982).
- [28] A.W. Fliflet and V. McKoy, *Phys. Rev. A* **21**, 1863 (1980).
- [29] M.-T. Lee and V. McKoy, *Phys. Rev. A* **28**, 697 (1983).
- [30] T. Nishimura and Y. Itikawa, *J. Phys. B* **27**, 2309 (1994).
- [31] J.O. Hirschfelder, C.F. Curtis, and R.B. Bird, *Molecular Theory of Gases and Liquids* (John Wiley, New York, 1954).
- [32] M.-T. Lee, L.E. Machado, and L.M. Brescansin, *J. Mol. Struct.: THEOCHEM* **464**, 79 (1999).
- [33] T. Sakae, S. Sumyoshi, E. Murakami, Y. Matsumoto, K. Ishibashi, and A. Katase, *J. Phys. B* **22**, 1385 (1989).
- [34] A. Zecca, G.P. Karwasz, and R.S. Brusa, *Phys. Rev. A* **45**, 2777 (1992).
- [35] H. Nishimura and T. Sakae, *Jpn. J. Appl. Phys., Part 1* **29**, 1372 (1990).
- [36] O. Sueoka and S. Mori, *J. Phys. B* **19**, 4035 (1986).
- [37] I. Kanik, S. Trajmar, and J.C. Nickel, *Chem. Phys. Lett.* **193**, 281 (1992).
- [38] M.-T. Lee, I. Iga, L.E. Machado, and L.M. Brescansin (unpublished).